OBSERVATION OF UNIDIRECTIONAL CURRENT RECTIFICATION AND AC-TO-DC POWER CONVERSION BY AS-GROWN SINGLE-WALLED CARBON NANOTUBE TRANSISTORS

Govind Mallick[*], Mark Griep, Samuel Hirsch, and Shashi P. Karna

Department of the Army, 4600 Deer Creek Loop, WMRD, ATTN: AMSRD-ARL-WM-BD, Army Research Laboratory, Aberdeen Proving Grounds, MD 21005, USA

Sarah Lastella, Sangeeta Sahoo and Pulickel M. Ajayan

Department of Materials Science and Engineering, Rensselaer Polytechnic Institute, Troy, New York 12180, USA

ABSTRACT

Current rectification property of chemical vapor deposited (CVD), as-grown single-walled carbon nanotube (SWNT) is investigated. The long strands of SWNT bundles are used to fabricate multiple arrays of switching devices with the channel length of 3, 5, 7 and 10 μm on a 15 mm x 15 mm SiO_2 on Si substrate. The majority of the fabricated devices, regardless of their channel length, show current rectification characteristics with high throughput of current (I) in the forward bias (V). Atomic force microscopic (AFM) analysis of the device structure and surface topology of SWNT suggest the observed rectification of current to result from surface irregularities and possibly due to change in the chirality of a single tube. Utilizing the fabricated SWNT FETs for the first time, a nanoscale AC-to-DC power converter is demonstrated.

KEYWORDS

Single-walled carbon nanotube, current rectification, diode, AC-to-DC power converter

1. INTRODUCTION

Current rectification by single-walled carbon nanotubes (SWNT) has been predicted from theoretical calculations (Trebaux et. al, 1999; Srivastava et. al., 2003) and has also been observed in a number of previous experiments (Collins et. al., 1997; Satishkumar et. al., 2000; Zhou et. al., 2000, Lee et al., 2004). Theoretical predictions suggest the cross or Y-type junctions, atomic defect, and/or changes in chirality along the tube axis can lead to current rectification due to Schottky – type junctions.

Experimental observations have been made on Y-type junctions (Satishkumar et. al., 2000) with tubes having different diameters forming the junction, chemical doping of the tubes (Zhou et. al., 2000), as well as double-gate electrostatic doping of tubes (Lee et al., 2004), effectively creating p-n junction along a single tube.

Rectifiers have important applications in military as well as commercial electronics as radio signal detectors and AC-to-DC power converter. In order to realize nanoscale electronics and microsystems, it is critically important to develop materials and establish mechanisms for nanoscale current rectification. As a first step toward realizing nanoscale rectifiers, we have investigated the I – V characteristics of CVD-grown, SWNT field-effect transistors (FETs). Here we present the results of our study showing current rectification by "as-grown" SWNT devices without external doping. We propose the diode-like property due to the hybrid chirality of single tubes.

The electronic structure of the nanotubes depend on their diameter and helicity (Saito et. al., 1992; Hamada et. al., 1992). They can be either metallic or semiconducting depending on the arrangements of the phenyl rings. The arm-chair CNTs are metallic whereas the zig-zag can be either metallic (1/3) or semiconducting (2/3) (Wildöer et. al., 1998; Odom et. al., 1998). Theoretically it is possible that these different helices can be joined together in a single wall nanotube through a linear junction and hence creating a diode-like property (Treboux et. al., 1999; Chico et. al., 1996). In general, diode-like behavior in nanotubes is caused by creating an energy barrier at the junction by the change in the internal structure of the tube. However, this type of behavior is seldom seen in CVD processed CNTs. Typically they show either a metallic or semi-conductive behavior (Lastella et. al., 2006; Lastella et. al., 2004). Here we report

Report Documentation Page

Form Approved
OMB No. 0704-0188

Public reporting burden for the collection of information is estimated to average 1 hour per response, including the time for reviewing instructions, searching existing data sources, gathering and maintaining the data needed, and completing and reviewing the collection of information. Send comments regarding this burden estimate or any other aspect of this collection of information, including suggestions for reducing this burden, to Washington Headquarters Services, Directorate for Information Operations and Reports, 1215 Jefferson Davis Highway, Suite 1204, Arlington VA 22202-4302. Respondents should be aware that notwithstanding any other provision of law, no person shall be subject to a penalty for failing to comply with a collection of information if it does not display a currently valid OMB control number.

1. REPORT DATE	2. REPORT TYPE	3. DATES COVERED
DEC 2008	**N/A**	**-**

4. TITLE AND SUBTITLE	5a. CONTRACT NUMBER
Observation OF Unidirectional Current Rectification And AC-TO-DC POWER Coversion BY AS-GROW Single-WALLED Carbon Nanotube Transistors	5b. GRANT NUMBER
	5c. PROGRAM ELEMENT NUMBER

6. AUTHOR(S)	5d. PROJECT NUMBER
	5e. TASK NUMBER
	5f. WORK UNIT NUMBER

7. PERFORMING ORGANIZATION NAME(S) AND ADDRESS(ES)	8. PERFORMING ORGANIZATION REPORT NUMBER
Department of the Army, 4600 Deer Creek Loop, WMRD, ATTN: AMSRD-ARL-WM-BD, Army Research Laboratory, Aberdeen Proving Grounds, MD 21005, USA	

9. SPONSORING/MONITORING AGENCY NAME(S) AND ADDRESS(ES)	10. SPONSOR/MONITOR'S ACRONYM(S)
	11. SPONSOR/MONITOR'S REPORT NUMBER(S)

12. DISTRIBUTION/AVAILABILITY STATEMENT
Approved for public release, distribution unlimited

13. SUPPLEMENTARY NOTES
See also ADM002187. Proceedings of the Army Science Conference (26th) Held in Orlando, Florida on 1-4 December 2008, The original document contains color images.

14. ABSTRACT

15. SUBJECT TERMS

16. SECURITY CLASSIFICATION OF:			17. LIMITATION OF ABSTRACT	18. NUMBER OF PAGES	19a. NAME OF RESPONSIBLE PERSON
a. REPORT **unclassified**	b. ABSTRACT **unclassified**	c. THIS PAGE **unclassified**	**UU**	**5**	

Standard Form 298 (Rev. 8-98)
Prescribed by ANSI Std Z39-18

asymmetric/diode behavior in the I – V characteristics of CVD grown SWNTs, possibly due to the internal defects.

2. MATERIALS AND METHODS

SWNTs are grown using metal nanoparticle catalyzed CVD process (Lastella et. al., 2004). The CNT-CVD synthesis procedure utilizes methane (CH_4) gas as the feedstock carbon source. Fe-nanoparticles are used as the catalyst for CNT growth. A Fe-nanoparticle coated 100 nm thick silicon oxide layer on heavily-doped silicon is used as the substrate. The catalyst nanoparticle coated substrate is placed inside the tube oven and heated to 920°C under a constant argon flow (~50 sccm) and pressure of 500 Torr. Upon reaching the set-point temperature, the system is maintained at these conditions for 10 minutes to ensure that the environment inside the tube furnace is stable. Finally, the argon flow is turned off and the methane flow is simultaneously initiated at a rate of ~100 sccm. After 5 minutes, the growth is ceased by turning off the methane flow, evacuating the system to 200 mTorr and allowing the system to cool to room temperature over a period of 2.5 hours. This CVD technique coupled with a novel catalyst system allows relative control of the nanotube properties and alignment such that the final product could be easily converted into a working device. Surface characterizations of the as grown SWNT samples are performed by AFM (CP-II, Veeco).
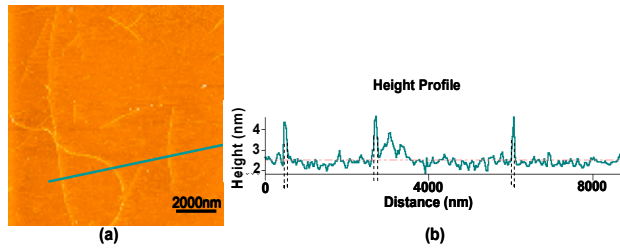

Fig. 1. (a) AFM topographical image (10 μm x 10 μm) of as-grown chemical vapor deposited SWNTs and (b) the related height profile.

The devices are fabricated by photolithographically depositing a 100 nm layer of Au on top of 10 nm thick Ti to serve as electrodes with varying source (S) and drain (D) separation. The dimension of each electrode pad is 250 μm x 250 μm. Each device is uniquely labeled, distinguishing its channel length and its respective row and column. The samples are then annealed at 200°C for 30 minutes in constant flow of nitrogen to eliminate possible oxide defects. The post-fabricated devices are analyzed by scanning electron microscope (SEM: Hitachi S-4700) to investigate the structure of the devices and the gaps between the electrodes while AFM is used to locate the bridging carbon nanotubes between the electrodes under ambient conditions. We are able to locate bundles

of SWNT connecting the pads with all four gap devices. A single substrate with an approximate size of 15 mm x 15 mm comfortably houses 135 devices. These include four different types with a channel length (gap) between the electrodes of 3, 5, 7, and 10 μm, respectively. The electrical properties of the assembled devices are probed by utilizing I – V measurements with a semiconductor (SC) analyzer (Janis/Keithley-4200) attached to a four-probe micro manipulated cryogenic system.

The AC/DC conversion properties of the SWNT devices are also explored on the SC analyzer (Janis/Keithley-4200) using the four-probe micro manipulators to make contact with the device source/drain pads. The source pad of the SWNT pad is wired to a pulse generator (Agilent 81110) to provide an AC input signal of controlled frequency, amplitude, and waveform. For lower input frequencies, < 1 Hz, the drain pad of the SWNT device is connected to the SC analyzer for measurement of the output signal. At higher input frequencies it was necessary to perform the output measurements on a high sampling rate oscilloscope (Agilent 54621A, 1 MΩ input resistance).
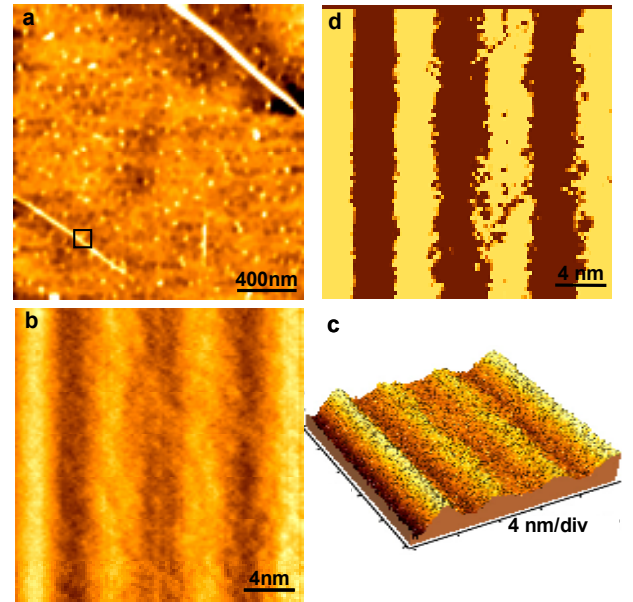
RESULTS AND DISCUSSIONS

Fig. 2. (a) AFM topographical image of 2 μm x 2 μm scan area, (b) partial atomic resolution AFM topographical image of the area indicated in (a), (c) 3D image of (b) and (d) filtered image of (b) differentiating the topography in two color regime showing the defects in SWNTs.

Fig. 1 (a) and (b) presents the AFM image and height profile of as-grown SWNTs on a 10 μm x 10 μm Si/SiO_2 substrate. As indicated by the height profile, the SWNTs are 2 to 3 nm in height which corresponds to the

2

approximate known diameter of SWNTs. Interestingly, the width of the imaged SWNTs is found to be ~100 nm, indicating aligned bundles of SWNT. Atomic resolution images of part of the nanotube, shown in Fig. 2, reveals that each CNT strand shown in Fig. 1 is, in fact, a bundle of several single nanotubes aligned parallel to each other. For one segment (Fig 2a) of a nanotube bundle, the AFM scan shown in Fig. 2 (b, c & d) exhibit four individual nanotubes aligned parallel to each other, with individual diameter of ~2 nm each in a scan area of 20 nm x 20 nm. In Fig. 2b the first tube displays smooth and cylindrical walls, while the three remaining tubes are distorted and exhibit discontinuity on the tube wall. This is made clear in Fig. 2d, which is the height image of Fig. 2b in terms of two color regimes. A closer examination of the two central tubes in Fig. 2b further reveals that the tubes are twisted on their respective axis. As described by Dumitrica et al, (Dumitrica et. al., 2006) the bonds of nanotubes can either snap in a brittle fashion or they may stretch and deform. However, the intrinsic properties of the tubes play a major role in the breakage. For example, the intrinsic twist or chirality of the tube can create strain and stress to the neighboring bonds, resulting in bond cleavage.

Some of the devices, specifically those near the edges of the substrate are damaged and could not be probed. Of the 135 fabricated devices, 103 are probed, of which 35% are found to be active in this particular sample. Out of these active devices 61% of 3 μm-gap, 28% of 5 μm-gap, 22% of 7 μm-gap and 26% of 10 μm-gap devices are found active, i.e. they show measurable electrical characteristics. A majority of the active devices (72%) show asymmetric I – V curves and rest are either metallic or have no observable electrical activity due to lack of connecting tubes.
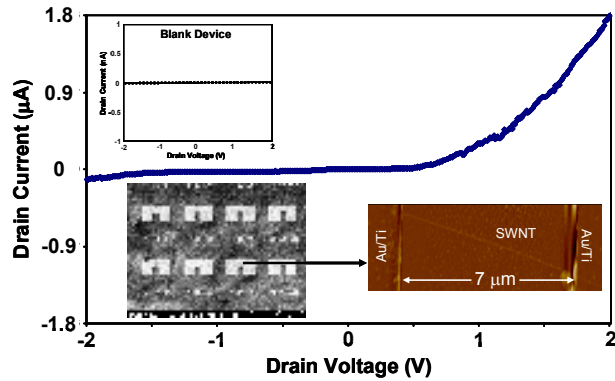
Fig. 3. Two-terminal I - V measurement of 7 μm-gap device. The lower inset shows the SEM image of different device patterns and an AFM image of 2.5 μm x 10 μm scan area showing SWNTs connecting the two electrode pads. The upper left inset shows the I - V measurement of a blank 7 μm-gap device.

A typical I – V curve of a fabricated SWNT device obtained from a two-probe measurement is shown in Fig.

3. The I – V curve shown is for a 7 μm channel length device (lower inset). The upper inset is the I – V curve on a 7 μm length control device with no SWNT in the channel. The left lower inset shows the scanning electron micrograph of the device layout. Furthermore, the SWNT diodes give high throughput of current in the forward bias (Fig. 3). The forward/reverse current ratio (I_{for}/I_{rev}) is in the order of 10^6. The asymmetric behavior is possibly due to the internal defect, as shown in Fig. 4 which is the exposed atomic resolution image of second strand of SWNT bundle in Fig. 2. The analysis reveals that the tube is twisted significantly. Here a part of the graphene sheet as a layer of nanotube wall is super imposed on the AFM atomic resolution image. This shows the distinction where one part of the sheet has armchair (n,n) chirality and the other part is zig-zag (n,0). This chirality alteration is most likely due to the twisting of the nanotube. It is a well documented fact that the armchair tubes have virtually negligible energy gap compared to the zig-zag (Ouyang et. al., 2001). Thus a tube with mixed chirality gives rise to a potential barrier at the junction of the dissimilar chiral structures, resulting in asymmetric current under biased condition.
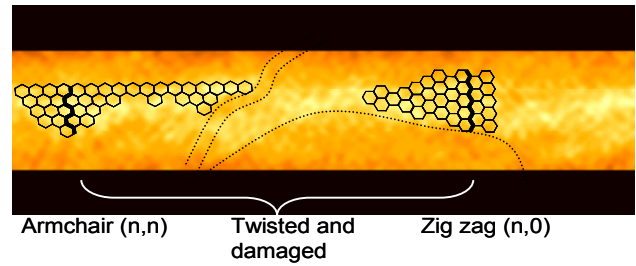
Fig. 4. Atomically resolved AFM image (10 nm x 2 nm) of a single strand of SWNT. The dotted lines show the twisting and possible fragments of bonds.

Possibility of unimolecular SWNT diode has been discussed in previous studies (Srivastave et. al., 2003; Collins et. al., 1997; Satishkumar et. al., 2000; Zhou et. al., 2000). Since our devices also consist cross junctions with varying tube diameters (AFM image, not shown here) along different arms as well as bundles with mixed metallic-semiconducting tubes it is important to consider the possible mechanism of the observed rectification – notably the cross-junctions of tubes with metallic and semi-conducting properties, contributions due to tube electrode junctions and single tubes with morphological non-uniformity including atomic level defects, tube wall deformation and mixed chirality along the tube length. We can not conclusively exclude the contributions from cross-junction tubes due to the observed presence of such junctions in some of our devices. However, since our device use symmetric electrodes (Au on both sides) we may exclude the effect of dissimilar electrodes. Due to the same reason (symmetric electrode), we believe that the difference in tube electrode contact resistance at the two junctions has little or no contribution to the observed rectification. This leaves us with the possibility of a

Schottky diode with channels consisting of SWNTs with different work functions and possibly different electronic structure.

The current and its voltage derivative (conductance) as a function of applied voltage dominant diode type SWNT devices fabricated in this study are summarized in Fig. 5 (a) and (b), respectively. It is clearly seen that the magnitude of the drain current is significantly higher at the positive bias compared to the negative bias indicating pure diode properties of the devices. The open device architecture used in the present work has led us to explore the new regime and properties of SWNTs.
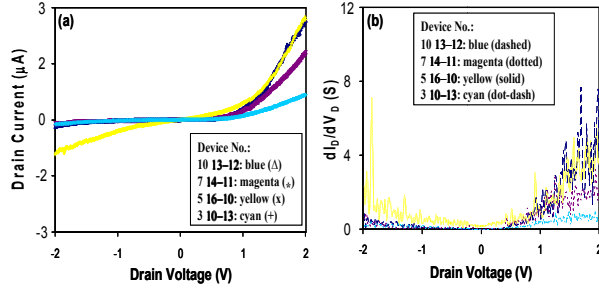
Fig. 5. (a) Two-terminal I - V measurements of four different gap devices and (b) their respective conductance plot.

The present research also opens new application areas for SWNT-based devices such as AC to DC power conversion in high-power electronics. Initial studies on the current SWNT-based devices demonstrate the ability to perform half-wave power conversion, as shown in a virtual rectifying region of semiconducting sample displayed in Fig. 6. With a 4 V peak-to-peak AC input signal set at 1 Hz, offset +0.5 V to demonstrate rectification as shown in Fig. 6(a), the ability to produce a DC-output is demonstrated in Fig. 6(b). It can be seen that the entire negative voltage component of the input signal is cut-off and only the positive input is passed through the SWNT-device, thus creating a half-wave AC-to-DC power conversion.
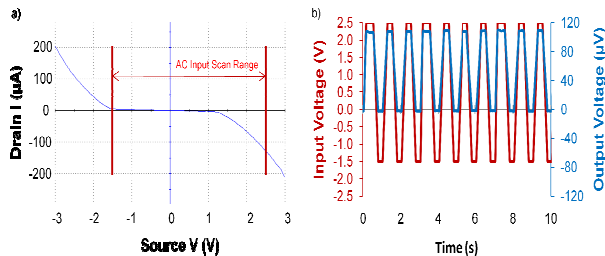
Fig. 6. (a) The I - V trace of a sample revealing semi-conducting behavior and (b) corresponding AC/DC half-wave conversion of a 4 V p-p amplitude 1 Hz AC input, offset 0.5 V to simulate rectification behavior.

Further studies were performed on another sample that showed rectification behavior shown in Fig. 7(a), to evaluate power conversion characteristics at higher input

frequencies. It can be seen that the I - V characteristics allowed approximately 3.5 times the electron flow when positive 1 V is applied, as opposed to the current output seen at negative 1 V. With a 1 MΩ input resistance on the oscilloscope the output voltage from a +/-1 V input can be estimated, as also displayed in Fig. 7(a). The AC to DC conversion characteristics of this device can be seen to directly relate to the current flow displayed in the I - V curve, thus a +/-1 V input signal produces approximately 3.5 times the output voltage in the positive direction as compared to the negative voltage output as displayed in Fig. 7(b). The AC to DC conversion characteristics of this device remained relatively constant over a tested range of 1 Hz to 60 Hz as displayed in Fig. 8. All output values closely matched the theoretical values determined from the SWNT I - V characteristics, thus demonstrating the ability of using SWNT devices to perform AC to DC power conversion.
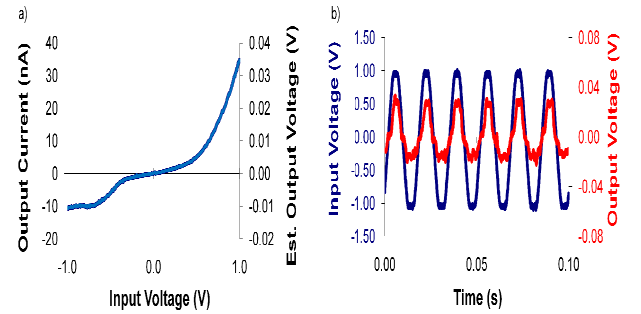
Fig. 7. (a) The I - V trace revealing rectification behavior along with the estimated DC voltage output through a 1 MΩ input resistance oscilloscope. (b) Experimental AC/DC half-wave conversion of a 1 V amplitude 60 Hz AC input.
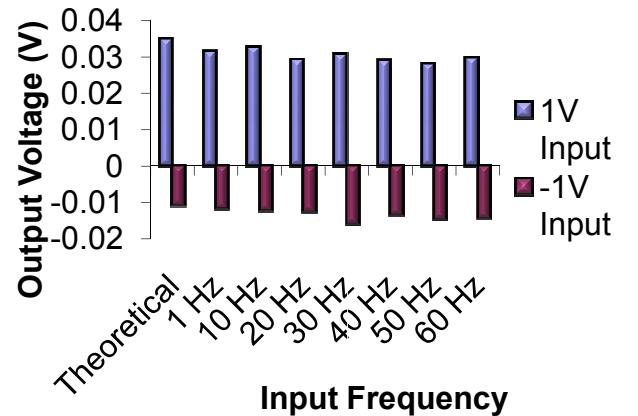
Fig. 8. AC/DC half-wave conversion characteristics remained consistent over a range of input frequencies (1V AC input).

CONCLUSION

We have grown SWNT by CVD process and fabricated arrays of SWNT electronic switches in open channel configurations. A large majority of the devices fabricated

4

with the "as-grown" SWNT exhibit prominent rectification characteristics (I_{for}/I_{rev} ~10^6), which have demonstrated the ability to serve as half-wave AC to DC power conversion devices. We have also demonstrated the fabrication of arrayed patterns of SWNT switching devices on a single chip. The process is compatible with the current industry-standard Si-electronics and could be easily transitioned for mass fabrication of the SWNT switching devices. The SWNT transistors exhibit the ability to serve as half-wave power converters, displaying this property over a wide-range of input frequencies with input voltage of +/-3 V. The half-wave output closely matches theoretical output voltages. This is the first ever observation of AC-to-DC conversion by SWNT FETs.

REFERENCES

[1] G. Treboux, P. Lapstun, and K. Silverbrook, "An Intrinsic Carbon Nanotube Heterojunction Diodes," *J. Phys. Chem. B*, v. 103, pp. 1871-1875, 1999.

[2] D. Srivastava, M. Menon, and P. M. Ajayan, "Branched Carbon Nanotube Junctions Predicted by Computational Nanotechnology and Fabricated through nanowelding," *J. Nanoparticle Res.*, v. 5, pp. 395-400, 2003.

[3] P. G. Collins, A. Zettl, H. Bando, A. Thess, and R. E. Smalley, "Nanotube Nanodevice," *Science*, v. 278, pp. 100-103, 1997.

[4] B. C. Satishkumar, P. J. Thomas, A. Govindraj, and C. N. R. Rao, "Y-Junction Carbon Nanotubes," *Appl. Phys. Lett.*, v. 77, pp. 2530-2532, 2000.

[5] C. Zhou, J. Kong, E. Yenilmez, and H. Dai, "Modulated Chemical Doping of Individual Carbon Nanotubes," *Science*, v. 290, pp. 1552-1555, 2000.

[6] J. U. Lee, P. P. Gipp, and C. M. Heller, "Carbon Nanotube p-n Junction Diodes," *Appl. Phys. Lett.*, v. 85, pp. 145-147, 2004.

[7] R. Saito, M. Fujita, G. Dresselhaus and M. S. Dresselhaus, "Electronic Structure of Chiral Graphene Tubules," *Appl. Phys. Lett*. v. 60, pp. 2204-2206, 1992.

[8] N. Hamada, S. Sawada and A. Oshiyama, "New One-Dimensional Conductors: Graphitic Microtubules," *Phys. Rev. Lett*. v. 68, pp. 1579-1581, 1992.

[9] J. W. G. Wildöer, L. C. Venema, A. R. Rinzler, R. E. Smalley and C. Dekker, "Electronic Structure of Atomically Resolved Nanotubes," *Nature,* v. 391, pp 59-62, 1998.

[10] T. W. Odom, J. Huang, P. Kim and C. M. Lieber, "Atomic Structure and Electronic Properties of Single-Walled Carbon Nanotubes," *Nature*, v. 391, pp. 62-64, 1998.

[11] L. Chico, V. H. Crespi, L. X. Benedict, S. G. Louie and M. L. Cohen, "Pure Carbon Nanoscale Devices: Nanotube Heterojunctions," *Phys. Rev. Lett*. v. 76, pp. 971-974, 1996.

[12] S. Lastella, G. Mallick, R. Woo, D. A. Rider, I. Manners, Y. J. Jung, C. Y. Ryu, P. M. Ajayan and S. P. Karna, "Parallel Arrays of Individually Addressable Single-Walled Carbon Nanotube Field-Effect Transistor," *J. Appl. Phys*. v. 99, pp. 024302 (1)-024302 (4), 2006.

[13] S. Lastella, Y. Joon Jung, H. Yang, R. Vajtai, P. M. Ajayan, C. Y. Ryu, D. A. Rider and I. Manners, "Density control of single-walled carbon nanotubes using patterned iron nanoparticle catalysts derived from phaseseparated thin films of a polyferrocene block copolymer," *J. Mat. Chem.*, v. 14, pp. 1791-1794, 2004.

[14] P. Dumitrica, M. Hua and B. I. Yakobson, "Symmetry-, Time-, and Temperature-Dependent Strength of Carbon Nanotube," *Proceedings of National Academy of Sciences (PNAS)*, v. 103 (16), pp. 6105-6109, 2006.

[15] M. Ouyang, J. Huang, C. L. Cheung and C. M. Lieber, "Atomically Resolved Single-Walled Carbon Nanotube Intramolecular Junction," *Science*, v. 292, pp. 97-100, 2001.